Research Paper | Open Access

Structure and Surface Characterization of Nanostructured Tio₂ Coatings Deposited Via HVOF Thermal Spray Processes

[1,]Maryamossadat Bozorgtabar , [2,]Mohammadreza Jafarpour
[a] *Department of Materials Engineering, Majlesi Branch, Islamic Azad University, Isfahan, Iran.*
[b] *Mobarakeh Steel Company, Isfahan, Iran*

ABSTRACT : *Titanium dioxide coatings were deposited by high velocity oxy-fuel spraying (HVOF) with the use of agglomerated P25/20 nano-powder and different spraying parameters (e.g. fuel/flow ratio) to determine their influence on the microstructure, crystalline structure and surface feature of the coatings. The microstructure of as-sprayed TiO_2 coatings was characterized by scanning electron microscope (SEM), transmission electron microscope (TEM) and X-ray diffraction (XRD). Surface features were investigated by Fourier transform infrared (FT-IR) and X-ray photoelectron spectroscopy (XPS). The results showed that the fuel and oxygen flow ratio have an important influence on the microstructure, anatase content, surface chemical state and surface feature of the TiO_2 coatings.*

KEY WORDS: *Nano materials; Coatings; Microstructure; TiO_2; Thermal Spray; XPS.*

I.   INTRODUCTION

Titanium dioxide (TiO_2), since the first report of the Honda–Fujishima effect, has received great attention in a range of scientific and industrial fields, such as light-induced water splitting, dye-sensitized solar cell and self-cleaning surfaces [1, 2]. Due to its unique electronic, photo-electronic and catalytic properties Photo-degradation of an organic contaminant becomes one of the most important applications of TiO_2, which is a fast-growing research area in recent years [3, 4]. In order to increase TiO_2 application activity, many methods are put forward, such as selecting TiO_2 nano-crystalline particles [5, 6]. So far, a vast amount of energy and effort has already been devoted to this subject by researchers. Now it seems to be the right time to find more practical ways to use the technology on an industrial scale. Crystal structure and surface characteristics of TiO_2 play an important role in its many applications, and this article addresses their importance in the expanded use of TiO_2. Among the two TiO_2 crystalline phases, anatase and rutile that can contribute to the photo-catalysis, it is generally assumed that the anatase, the metastable phase which by thermal treatment irreversibly turns into rutile, allows a higher-photo-catalytic degradation of the pollutants. However, some anatase powders containing small quantities of rutile present a better efficiency than those of pure anatase [7]. For example, titanium dioxide can be used in powder form (slurry) or immobilized in a thin film or coating form obtained by different deposition techniques (thermal spray, sol-gel, dip-coating, and physical or chemical vapor deposition, etc.) [8, 9].

Among coating procedures, thermal spray is characterized as a flexible and efficient process which has been widely used to deposit both metallic and non-metallic coatings. The thermal spraying process has many advantages, including its low cost, formation of thicker coatings quickly, a wide selection of materials and a process that is much simpler than other coating processes [10]. Thus thermal spraying is considered to be the optimal method for producing TiO_2 coatings in most industrial applications [11]. During thermal spraying, powders are heated and accelerated and then projected on to a substrate, followed by flattening, rapid cooling and a solidification process, which results in a typical quenched microstructure. Thermal spray processing is a commercially relevant, proven technique for processing nano-structured coatings [12, 13]. Thermal spray techniques are effective because agglomerated nano-crystalline powders are melted, accelerated and impacted against a substrate, and quenched very rapidly in a single step. This rapid melting and solidification promotes the retention of the nano-crystalline phase and produces a uniform amorphous structure. Retention of the nano-crystalline structure leads to enhanced wear behavior, greater hardness, and sometimes a reduced coefficient of friction compared to conventional coatings [12, 13].

The investigation on TiO_2 coatings deposited through conventional flame spraying and plasma spraying showed that the coatings consisted mainly of the rutile phase with only a low fraction of anatase phase, despite the crystalline structure of the initial powders. The anatase content in the coatings was around 10 to 15% deposited with the spray powder at a well-melted condition regardless of the spray powders original crystalline structure [14, 15]. Toma et al. [16] have reported that the coating with 12.6% by volume anatase content could be deposited through a gas fuel high velocity oxy-fuel (HVOF) spray when TiO_2 powder in the anatase phase was used as feedstock. Yang et al. [17] have reported an anatase content of 35% by volume and 55% by volume was achieved in the gas fuel HVOF coating deposited with rutile and anatase powder. In this research, the coatings were deposited through a liquid fuel high velocity oxy-fuel spray with different fuel and oxygen flow ratio using TiO_2 nano-powders containing anatase and rutile as feedstock. The influence of the fuel and oxygen flow ratio on anatase content ratio, crystal size, morphology of the coating, surface chemical state and surface feature were investigated accordingly.

II. MATERIALS AND EXPERIMENTAL ASSESSMENT

Materials: P25/20 TiO_2 nanopowders were used as the feedstock for coating deposition. The powder used in this research was a commercially agglomerated and granulated nano-powders with an average agglomerated size of 20 µm, containing both anatase and rutile phases. 5×50×50 mm stainless steel plate was employed as a substrate for the coating deposition. Prior to the spraying process, the substrate was blasted with silicon carbide grit in order to increase the adhesive strength of the coating to the substrate.

Coating Deposition : The Met Jet III High velocity oxy-fuel (HVOF) gun was used to spray coatings at a stand-off distance of 336 mm. Kerosene was used as a liquid fuel. The powder feed rate was fixed at 8 g/min and the powder was carried to the HVOF flame by N_2 at a flow rate of 4 l/min, through a nozzle diameter of 11 mm. During the spraying, the flow of fuel and oxygen was altered incrementally to control the heating condition of the spray powders and thus provide a measure of the heating effectiveness of the fuel/oxygen ratio. Table I summarized the spray condition of the coatings.

Characterization :

X-Ray Diffraction: X-rays diffraction (performed with a Philips PW3710 diffractometer) using Cu Ka radiation was employed to determine the anatase-to-rutile ratio in the feedstock powder and HVOF sprayed coatings. Scan step was 0.02°/sec with a step time of 0.5sec in the 20 –70° 2θ range. The volume percentage of anatase was determined according to the following relation [18]:

$$A = \frac{1}{1+1.265\frac{IR}{IA}} \times 100 \quad (1)$$

Where IA and IR are the X-ray intensities of the anatase (101) and the rutile (110) peaks, respectively. The crystallite size was evaluated from the X-ray diffraction patterns based on the Scherrer formula as shown in the following equation [18]:

$$t = \frac{0.9\lambda}{B\cos\theta} \quad (2)$$

With B = corrected peak width at half maximum intensity, λ = X-ray wavelength and   θ = Bragg diffraction angle.

Scanning and Transmission Electron Microscopy: The morphology of the feedstock powder and the microstructures of the coatings were examined using S360 Cambridge scanning electron microscope (SEM). TEM images were obtained using the LEO 912 transmission electron microscope that employed a tungsten electron gun in the voltage range of 120 kV with an optical point-to-point resolution of   1 nm. Samples were gently scraped from the substrate and examined by TEM.

FT-IR & X-Ray Photoelectron Spectroscopy : Infra-red spectra were recorded with a Fourier transform infra-red spectrometer (BRUKER, VECTOR33). Samples (gently scraped from the substrate) were carefully ground and diluted in non-absorbent KBr matrices (2-5 % by weight). All FT-IR spectra are shown in transmission units and obtained under atmospheric conditions. The chemical composition and valence state of the elements were carried out by X-ray photoelectron spectroscopy (VG Microtech, XR3E2) with an aluminum anode energy source at Ka = 1486.6 V. The pressure in the analysis chamber of the spectrometer was 10^{-9} mbar during acquisition. Binding energies were referenced to C1s (carbon contamination) at 285 eV.

III.   RESULTS AND DISCUSSION

Coatings crystalline structure : The crystalline structure of the elaborated HVOF-coatings was studied by XRD analysis. Fig 1 shows the XRD patterns of feedstock powder and coatings. It appears that the passage of the nano-particles in the flame involves a modification of their chemical state compared to the initial nano-powders, and which depends on the condition of the HVOF processes. The Fe peak is due to the effect from the iron in the SS substrate. Fig 2 shows the anatase content ratio of coatings. The C1 and C2 coatings, (obtained by 120 and 160 ml/min fuel flow rate and 800 l/min oxygen flow rate), contain anatase phases, with a ratio of about 80% by volume and 78% by volume respectively, which is more than the original feedstock powder content of 75% by volume. In contrast, the C3 and C4 deposited coatings, (with 120 and 160 ml/min fuel flow rate and 600 l/min oxygen flow rate), the ratio of anatase reached 36% by volume and 60% by volume respectively. It is clear that different fuel and oxygen flow rates cause different anatase-to-rutile phase transformation. As the fuel flow rate into the gun increases whilst the oxygen flow rate remains constant, the anatase content decreases, which cause a more significant explosion, result in higher torch temperatures. This higher explosion causes the torch velocity to increase due to the constant nozzle diameter, so by increasing fuel flow ratio, both the temperature and torch velocity has increased [19]. Higher fuel flow rate has thus resulted in higher velocities and temperatures and has also affected the anatase-rutile transformation and the retained anatase in the coating. By increasing the fuel flow rate, the gas velocity at the exit of the nozzle changed very little compared to the change in the gas temperature, [20] which (a) created more semi-molten particles, and (b) caused a lower solidification rate of particle droplet on the substrate, which consequently increased the rutile phase content in the coating. It is reported that rather than a constant fuel-to-oxygen ratio, the heat and velocity produced in the gas stream changes as the fuel and oxygen flow rate is varied, so that the results of coating with 800 and 600 l/min oxygen flow rates are significantly different.

Average anatase and rutile crystallite size of C1 to C4 coatings are shown in Fig. 3. In the C1, C2, C3 and C4 coatings, the anatase crystallite size reached 20.7, 25.9, 20.7 and 25.9 respectively from 25.9 nm of feedstock powder, in other words no change in C2 & C4 coatings while the rutile crystallite size reached 17.3, 17.3, 52.1 and 34.6 nm respectively from 41.7 nm feedstock powders. It is clear that different fuel and oxygen flow rates causes different changes in the crystallite size, and different changes in anatase and rutile crystallite size. The rutile crystallite size changed more than the anatase crystallite size. It is believed that in the thermal spray process, the formation of rutile is due to the molten particle and its slower solidification rate, while the formation of anatase is due to the anatase remaining in the primary particles, but also due to the rapid solidification rate of the molten particle on the substrate [21].Thus by changing the degree of melting of the particles in flight and also their solidification rate by changing the fuel and oxygen flow rate, changes in the anatase and rutile crystallite size can be obtained. With the higher fuel flow rate, there is a higher jet stream temperature and a higher degree of melting, so that the rutile crystallite size that forms from the molten droplets is also changed.

Coatings morphology : The SEM images of the surface and cross section microstructure of the C3 and C4 coatings can be observed in Fig.4 and Fig.5. The microscopic analysis showed that the morphologies of the sprayed coatings depend on the different coating conditions. The TiO_2 deposits have low porosity and are characterized by a layered microstructure, which can be observed in most thermally sprayed deposits. The coatings are built-up by the semi-melted and melted nano-particles impacting on the substrate that flatten to form splats, which consecutively pile on top of the others. In the C3 and C4 coatings, the semi-melted particles increase with the increase in the fuel flow rate. In the HVOF process, the velocity of the torch and in-flight particles are too high (about 1200 m/sec) and the temperature of torch is too low (about 2400° C) respectively, since this high speed causes very little heat to flow to the in-flight particles, therefore the degree of melting of the particles becomes too low [19]. Consequently, more semi-molten (molten surface and non-molten cores) particles contain higher amounts of anatase than fully molten particles can contain. [22]. By increasing the fuel flow ratio, the heat induced to the particles is increased, which in turn causes the ratio of semi-molten particles to non molten particles on the substrate to be increased.Fig.6 presents the typical TEM morphologies of the sprayed C1 coating. The size of most grains in the C1 coating is less than 30 nm with the average grain size being about 20 nm, which coincides with the grain size in the as-sprayed coatings measured by XRD.

Result of FT-IR and XPS: The FT-IR spectra of the feedstock powder, C1 to C4 sprayed coatings are shown in Fig. 7. For powder and coatings, the peaks at 460, 620 and 910/cm in the range of 400–1000/cm are contributions from the anatase TiO_2 [23, 24], which are also consistent with the observation from the XRD. Also it is believed that the broad peaks at 3400 and 1638/cm correspond to the surface-adsorbed water and hydroxyl groups [23,24]. The decrease in the intensities of these peaks in the FT-IR spectra of the C4 and C3 with larger anatase/rutile crystalline size was noted. Probably this was due to the decrease of specific surface areas which

caused the reduction of the adsorbed water. XPS analysis was mainly studied to evaluate the valence state of the titanium and the evolution of hydroxyl group on the TiO_2 surface [24]. Fig. 8(a) and (b) provides XPS spectra of the C1 coating, its titanium Ti2p and oxygen O1s and the results for O1s and Ti2p peaks. Six peaks of Ti2p1/2, Ti2p3/2, O1s, N1s, Fe2p3 and C1s were seen for the C1 coating. C1s peak at 284.6eV were organic polluted carbon used for calibration. The Fe peak is due to the substrate. Spectral data are summarized in Table II. For the TiO_2 sprayed coatings, the Ti2p peaks were identified at 458.5 and 463.9eV for Ti2p3/2 and Ti2p1/2 respectively, corresponding to Ti^{4+}; no reduction in the valence state of titanium was observed in the coating. The O1s spectrum displayed peaks at 529.5eV associated with $Ti–O^{(1)}$ bonds in TiO_2 (see Fig. 9), and at 530.3eV that corresponded to the hydroxyl ($Ti–O^{(2)}H$), and at 532eV related to chemisorbed water ($Ti–O^{(3)}H2$) [25, 26] as can be observed in the XPS spectra in Fig. 8(b). From results on O1s spectra in Table II, the amount of hydroxyl groups and water on the surface of the C1 coating was calculated, the ratio O/Ti was near the stoichiometric limit in the coating. Moreover, hydroxyl groups have a beneficial role in the photo-catalytic applications. It appears that the degradation of the pollutant was realized by the intermediate hydroxyl radicals formed by the reaction of the photo-generated holes with the hydroxyl groups or water chemisorbed on the surface. Indeed, a higher hydroxylation of the surface seemed to enhance the photo-catalytic activity of the TiO_2 [24]. Thus, the C1 coating presented an all-favorable surface characteristic to favor an increasing photo-catalytic behavior.

IV.   CONCLUSION

Titanium dioxide coatings were established by high velocity oxy-fuel spraying using kerosene fuel with Degussa P25/20 nano-powder as material feedstock. The microstructure, surface feature, crystal structure and surface chemical state of the samples were carefully analyzed, and from this analysis it clearly indicates that these features are strongly depended on the spray conditions. Phase composition changed from anatase in the powder to rutile in the as-sprayed coatings. A significant phase transformation from anatase to rutile occurred when the coatings were obtained by the higher fuel/flow ratio in the spray. The anatase phase was preserved in the coatings resulting from a lower fuel/flow ratio. Anatase and rutile crystallite size in the feedstock powder changed in the sprayed coatings. The change in the rutile crystallite size was greater than that of the anatase. The microstructure of the coatings was found to be dependent on fuel and oxygen flow ratios. In the higher fuel flow ratios, the melted zone is greater. It seems that the anatase content, anatase/rutile crystallite size and the microstructure are closely related to the flow rate of the fuel and oxygen. It is noted that the chemical composition of the coating is TiO_2, with correct stochiometry. The results showed that the surface of the coatings have adsorbed water and hydroxyl groups. It seems that the surface-adsorbed water and hydroxyl groups of coatings are dependent on the anatase/rutile crystallite size, since in the larger crystallite size they were reduced. It was found that the coating obtained under the lowest fuel/flow ratio with 800 l/min oxygen flow rate (C1), had the highest anatase content ratio (80%), the smallest crystallite size and showed the highest surface-water absorbed and hydroxyl groups that is important for its photo-catalytic function.

REFERENCES

[1]   Park IS, Choi SY, Ha JS .High-performance titanium dioxide photocatalyst on ordered mesoporous carbon support. Chem. Phys. Letters 2008; 456:198-201.
[2]   Demeestere K, Dewulf J, Witte BD, Beeldens A, Langenhove HV.Heterogeneous photocatalytic removal of toluene from air on building materials enriched with TiO_2. Building and Envi 2008; 43: 406-414.
[3]   Ma YS, Chang CN, Chiang YP, Sung HF, Chao AC. Photocatalytic degradation of lignin using Pt/TiO_2 as the catalyst. Chemosphere 2008; 71: 998-1004.
[4]   Yasomanee JP, Bandara J. Multi-electron storage of photoenergy using $Cu_2O–TiO_2$ thin film photocatalyst. Solar Energy Materials & Solar Cells 2008; 92:348-352.
[5]   Jensen H, Joensen KD, Jŕgensen JE, Pedersen JS, Sǵaard Egg. Characterization of nanosized partly crystalline photocatalysts. J. Nanoparticle Research 2004; 6:519-526.
[6]   Apátiga LM, Rubio E, Rivera E, Castaño VM. Surface morphology of nanostructured anatase thin films prepared by pulsed liquid injection MOCVD. Surf. Coat. Technol. 2006; 201: 4136-4138.
[7]   Iizuka Y, Kubo T, Nakahira A, Onodera D, Ozawa N, Yao T. Development of environmentally friendly photocatalyst with nano-size pore structure coated with thin Ti-oxide. Appl. Catalysis B: Envi. 2007; 76: 51–56.
[8]   Teoh WY, Amal R, Ma¨dler L, Pratsinis SE. Flame sprayed visible light-active $Fe-TiO_2$ for photomineralisation of oxalic acid. Catalysis Today 2007; 120:203-213.
[9]   Piera E, Ayllón JA, Doménech X, Peral J. TiO_2 deactivation during gas-phase photocatalytic oxidation of ethanol. Catalysis Today 2002; 76: 259-270.
[10]   Lima RS, Marple BR. Enhanced ductility in thermally sprayed titania coating synthesized using a nanostructured feedstock. Mater. Sci. Eng. A 2005; 395:269-280.
[11]   Berger-Kellera N, Bertrand G, Filiatre C, Meunierc C, Coddeta C. Microstructure of plasma-sprayed titania coatings deposited from spray dried Powder. Surf. Coat. Technol. 2003; 168: 281-290.
[12]   Ajayan PM, Schadler LS, Braun PV. Nanocomposite Science and Technology. Wiley; 2003.
[13]   Koch CC. Nanostructured Materials Processing, Properties and Potential Applications. New York; William Andrew Publishing Norwich: 2002.

[14]   Chwa SO, Klein D, Toma F L, Bertrand G, Liao H, Coddet C, Ohmori A. Microstructure and mechanical properties of plasma sprayed nanostructured TiO$_2$–Al composite coatings. Surf. Coat. Technol. 2005; 194:215- 224.

[15]   Kanazawa T, Ohmori A. Behavior of TiO$_2$ coating formation on PET plate by plasma spraying and evaluation of coating's photocatalytic activity. Surf. Coat. Technol. 2005; 197:45-50.

[16]   Toma FL, Bertrand G, Chwa SO, Klein D, Liao H, Meunier C, Coddet C. Microstructure and photocatalytic properties of nanostructured TiO$_2$ and TiO$_2$–Al coatings elaborated by HVOF spraying for the nitrogen oxides removal. Mater. Sci. Eng. A 2006; 417:56-62.

[17]   Yang G, Li C, Wang Y, Li C. Dominant microstructural feature over photocatalytic activity of high velocity oxy-fuel sprayed TiO$_2$ coating. Surf. Coat. Technol. 2007; 202: 63-68.

[18]   Spurr RA, Myers H. Quantitative Analysis of Anatase-Rutile Mixtures with an X-Ray Diffractometer. Anal. Chem. 1957; 29: 760-762.

[19]   Yanga GJ, Lia CJ, Hana F,Ohmori A. Microstructure and photocatalytic performance of high velocity oxy-fuel sprayed TiO$_2$ coatings. Thin Solid Films 2004; 466: 81- 85.

[20]   Li M, Christodes P D. Modeling and analysis of HVOF thermal spray process accounting for powder size distribution. Chem. Eng. Sci. 2003; 58: 849 - 857.

[21]   Yi Z, Wei W, Lee S, Jianhua G. Photocatalytic performance of plasma sprayed Pt-modified TiO$_2$ coatings under visible light irradiation. Catal. Commu. 2007; 8: 906-912.

[22]   Gaona M, Lima RS, Marple BR. Influence of particle temperature and velocity on the microstructure and mechanical behavior of high velocity oxy-fuel (HVOF)-sprayed nanostructured titania coatings. J. Mate. Processing Technol. 2008; 198: 426-435.

[23]   Xiaoa J, Penga T, Lia R, Penga Z, Yan C. Preparation, phase transformation and photocatalytic activities of cerium-doped mesoporous titania nanoparticles. J. Solid State Chem. 2006; 179:1161-1170.

[24]   Toma FL, Bertrand G, Begin S, Meunie C, Barres O, Klein D, Coddet C. Microstructure and environmental functionalities of TiO$_2$-supported photocatalysts obtained by suspension plasma spraying. Appl. Catal. B: Envi. 2006; 68:74-84.

[25]   Tai WP, Oh JHl Fabrication and humidity sensing properties of nanostructured TiO$_2$-SnO thin film. Sensores & Actuators B 2002; 85:152-157.

[26]   Backman U, Auvinen A, Jokiniemi JK. Deposition of nanostructured titania films by particle-assisted MOCVD. Surf. Coat. Technol.2005; 192: 81-87.
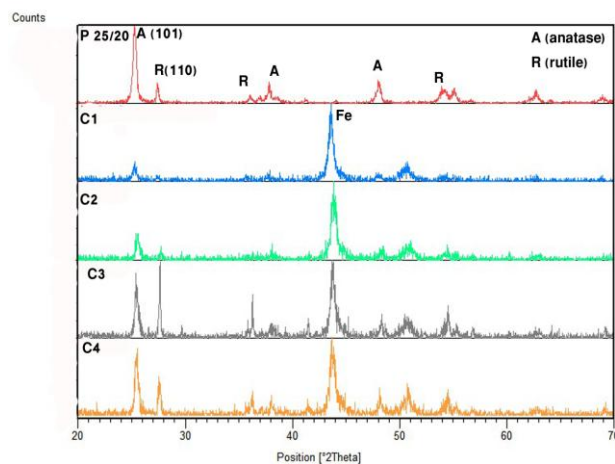
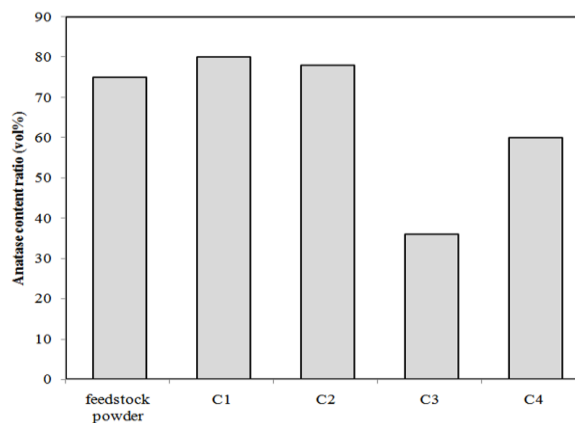Figure.1. XRD patterns of feedstock powder and TiO$_2$ sprayed coatings at different process parameters.

Figure.2. Anatase content ratio of TiO$_2$ sprayed coatings at different process parameters.
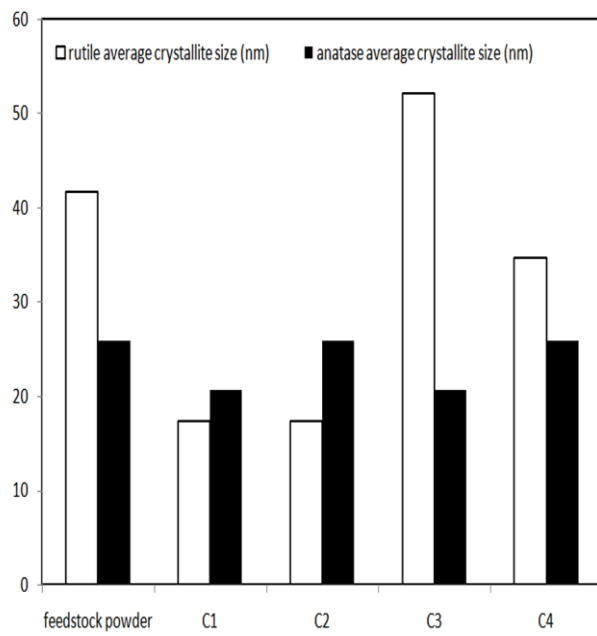
Figure.3. Rutile/anatase crystallite size of TiO$_2$ sprayed coatings at different process parameters.
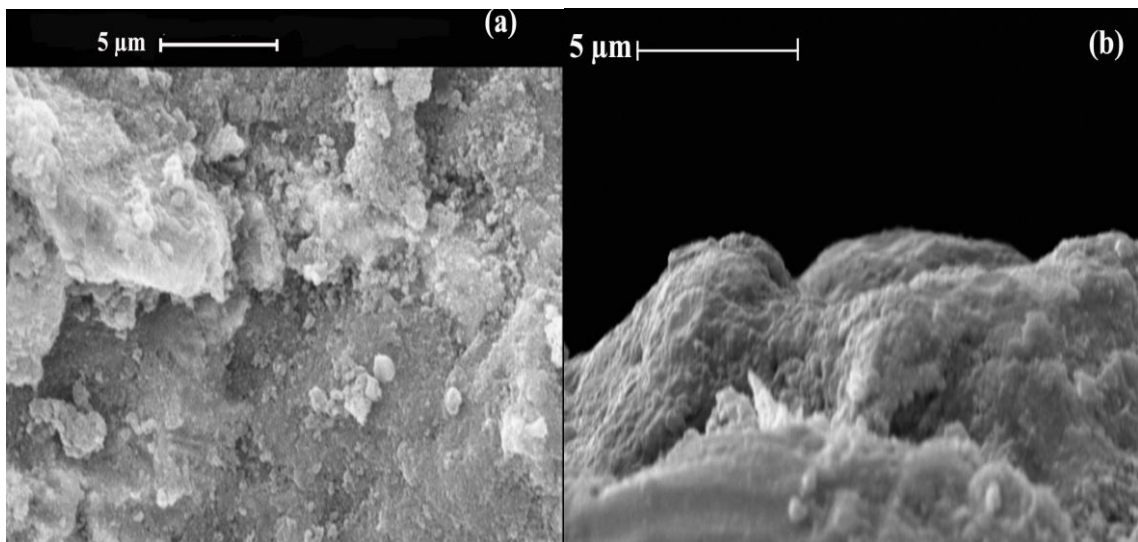

Figure.4. SEM images of (a) surface and (b) cross section of C3 Coating (Fuel flow rate: 160 ml/min, Oxygen flow rate: 600 l/min).
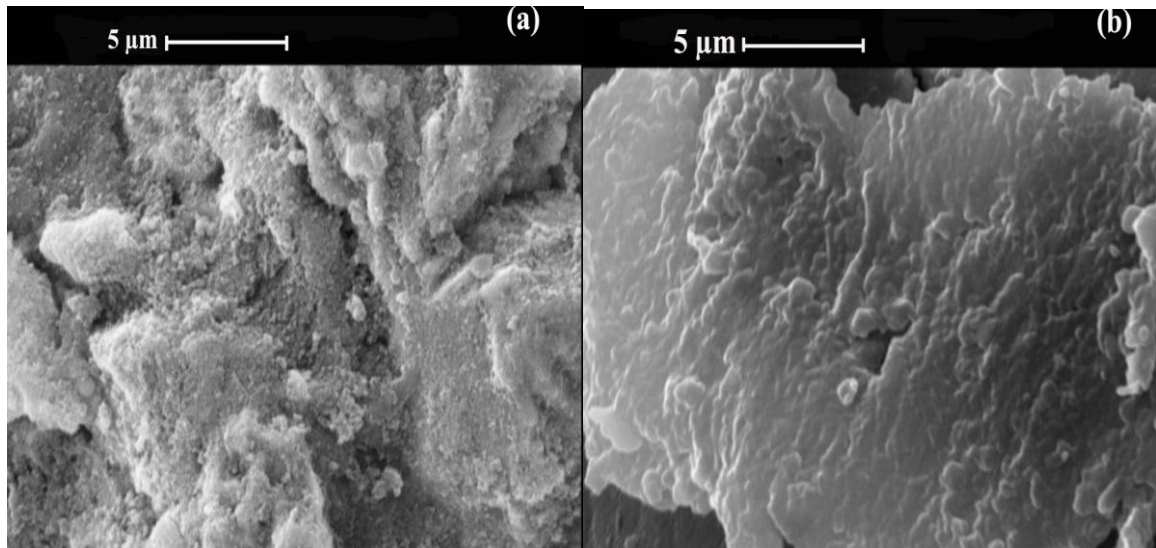
Figure.5. SEM images of (a) surface and (b) cross section of C4 Coating (Fuel flow rate: 120 ml/min, Oxygen flow rate: 600 l/min).
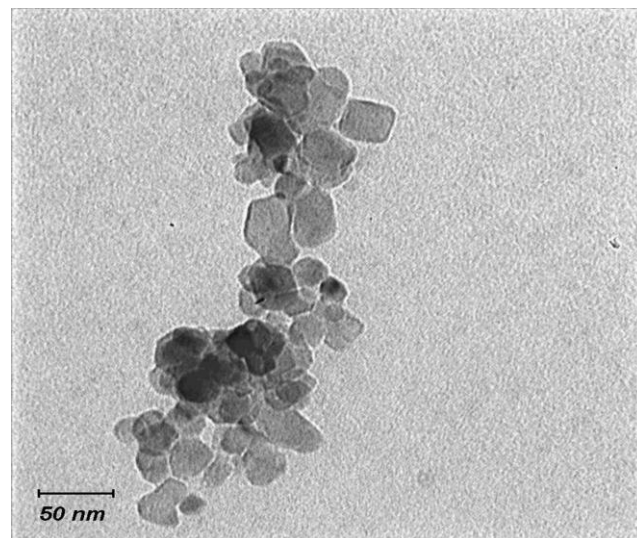

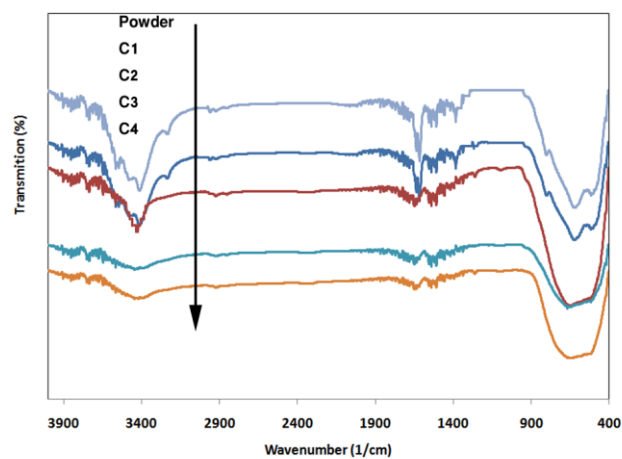Figure.6. TEM image of C1 coating (Fuel flow rate: 120 ml/min, Oxygen flow rate: 800 l/min).

Figure7. FT-IR patterns of feedstock powder and TiO_2 sprayed coatings at different process parameters.
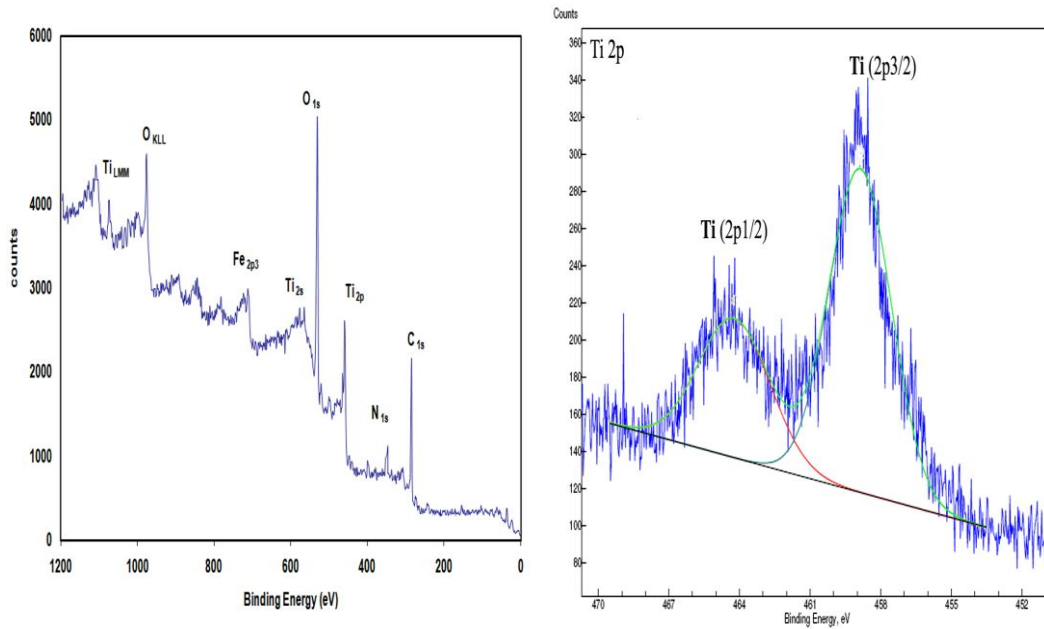
Figure.8. (a) XPS spectra of C1 coating, (b)Ti2p and O1s XPS spectra of C1 coating (Fuel flow rate:120 ml/min, Oxygen flow rate:800 l/min).
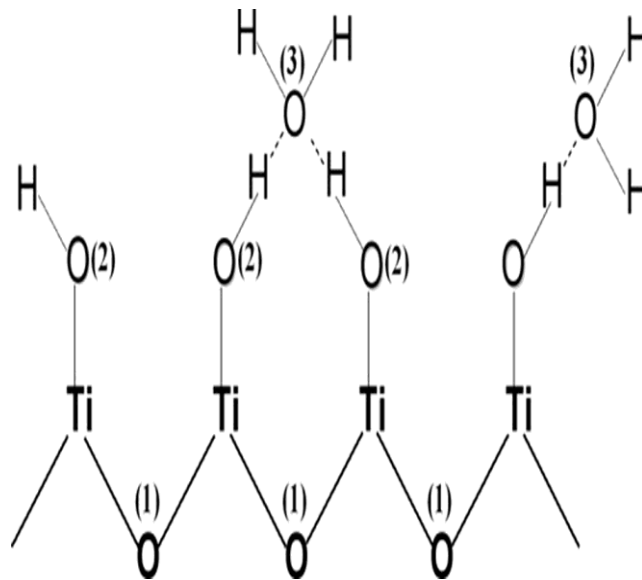

Figure.9. Schematic representation of the hydrated titanium dioxide surface.

Table I. Thermal spray parameters of TiO$_2$ coatings.

Samples	Fuel flow rate(ml/min)	Oxygen flow rate (l/min)
C1	120	800
C2	160	800
C3	160	600
C4	120	600

Table II. Binding energy values and oxygen species content for C1 sprayed coating (Fuel flow rate: 120 ml/min, Oxygen flow rate: 800 l/min).

C1 coating	Ti2p		O1s			$O^{(1)}/Ti \pm 0.2$
	Ti2p3/2	Ti2p1/2	Ti–$O^{(1)}$	Ti–$O^{(2)}$H	Ti–$O^{(3)}$H2	
Binding energy (eV)	458.5	464	529.5	530.8	532	2
Oxygen content (%) (±5)			71.1	18.5	10.4	